THE UNIVERSITY OF
WESTERN AUSTRALIA

Centre for Oil and Gas Engineering

Curtin
UNIVERSITY OF TECHNOLOGY

Center for Marine Science and Technology

Technical Report

Simulation of Ship Motions
– Coupled Heave, Pitch and Roll

By **Sheming Fan** and **Jinzhu Xia**

20 March, 2002

SUMMARY

The time-domain strip theory for vertical and rolling motions has been extended to predict the coupling of heave, pitch and roll motions by combining hydrostatic restoring force and moments in heave, pitch and roll displacements. Corresponding computer program is developed.

Time-domain simulations are performed for a Panamax Container ship at different headings and encounter frequencies. The coupling effect and parametric resonance are investigated.

It is seen that parametric instability occurs when the ship sails in quartering waves and very low encounter frequency. In other computational wave conditions, the effects of coupling of heave, pitch and roll are small.

CONTENTS

1. Introduction

The coupling motions of heave, pitch and roll have been discovered from both experimental observations and theoretical simulations. An extreme phenomenon is parametric resonance. In this case, the energy in heave and pitch motions may be transferred to roll motion mode through non-linear coupling, which leads to excessive resonant rolling and stability problems [1]. Excessive roll motion increases the probability of seasickness of the crew, reduces the operability of the onboard systems and, in the worst case, cause capsize of the vessel.

Because of the lateral symmetry of ship hull forms, linear theories are unable to account for the coupling between heave, pitch and roll. It is quite often that roll motion is treated as a single degree-of-freedom (DOF) dynamic problem, whereas heave and pitch are solved in a coupled two DOF system.

Some previous studies have employed simplified hydrodynamic models to simulate this problem. Hydrodynamic memory effect due to the free-surface wave motion is not incorporated, which give significant uncertainties in the simulations.

In other studies, the memory effect is expressed by a time convolution. The computation of time convolution limits the practical applications, and it is difficult to extend the theory to account for non-linear memory effects.

A rational non-linear time-domain hydroelastic strip theory was developed in [2] to predict vertical wave loads and ship responses. It was extended to compute anti-symmetric wave-induced ship response [3]. Both studies modeled the hydrodynamic memory effect by a higher-order differential approximation instead of time-consuming numerical integration. Hence the computational efficiency is maintained while the complicated non-linear phenomenon is investigated.

In the present research, the studies in [2] and [3] are merged to treat the coupling of roll motion with the vertical modes (heave and pitch) introduced by hydrostatic restoring forces and moments in heave, pitch and roll displacements. The coupled hydrostatic coefficients will be determined based on the instantaneous submerged area of each cross section and the integration over the ship length.

Time-domain simulations are performed for a Panamax Container ship at different headings and encounter frequencies.

2. Time-domain strip theory formulation [2, 3]

The Cartesian coordinate system (Figure 1) is defined as an 'equilibrium' set of axes translating with mean forward speed U of the ship in the $+x$-direction. The origin is at the stern. The $z=0$ plane corresponds to the calm water level, and z is positive upwards. The x-z plane is coincident with the plane of the ship hull.

The relative displacement between a ship section and wave surface can be expressed as

$$z_l(x,t) = w_l(x,t) - \xi_l(x,t) \qquad\qquad l = 2,3,4 \qquad\qquad (1)$$

where l=2 and 3 denote the lateral and vertical movements; l=4 denotes the rotation about the x-axis. $w_l(x,t)$ is the displacement component of ship section and $\xi_l(x,t)$ is the average displacement component of the wave at the ship section and is related to wave elevation with the Smith correction.

The time-domain sectional hydrodynamic force vector $\mathbf{F}(x,t)$ consisting of the lateral, vertical and rotational components without convolution may be expressed by [2, 3]

$$\mathbf{F}(x,t) = \frac{D\mathbf{I}}{Dt}$$

$$\sum_{j=0}^{J} (\mathbf{B}_j \mathbf{I} - \mathbf{A}_j \frac{D\mathbf{z}}{Dt})^{(j+1)} = 0 \qquad\qquad (2)$$

where $\mathbf{I}(x,t)$ represents both the impulsive and memory vectors in the hydrodynamic momentum; D/Dt is the total derivative with respect to time t, $\frac{D}{Dt} = (\frac{\partial}{\partial t} - U\frac{\partial}{\partial x})$ with U being the forward speed of the ship; $(\quad)^{(j)} = \frac{\partial^j}{\partial t^j}$; $\mathbf{A}_j(x)$ and $\mathbf{B}_j(x)$ are the so-called frequency-independent hydrodynamic coefficient matrices derived by a rational approximation from the frequency dependent added mass $\mathbf{m}(x,\omega)$ and damping coefficient $\mathbf{N}(x,\omega)$

$$i\omega m_{kl} - N_{kl} = \frac{\sum_{j=0}^{J} A_{j,kl}(-i\omega)^{j+1}}{\sum_{j=0}^{J} B_{j,kl}(-i\omega)^{j}} \qquad\qquad k,l = 2,3,4 \qquad\qquad (3)$$

where i is the imaginary unit and ω is the wave frequency.

Equation 2 can be extended empirically to include the non-linear loading effects due to the time variation of the wetted ship surface by assuming that the coefficients $\mathbf{A}_j(x)$ and $\mathbf{B}_j(x)$ vary with not only the longitudinal position but also the instantaneous submergence.

By integrating the higher-order differential equation in Equation 2, the sectional hydrodynamic force vector $\mathbf{F}(x,t)$ can be rewritten as

$$\mathbf{F}(x,t) = -\mathbf{m}\frac{D^2\mathbf{z}}{Dt^2} + U\frac{\partial \mathbf{m}}{\partial x}\frac{D\mathbf{z}}{Dt} - \frac{\partial \mathbf{m}}{\partial \mathbf{z}}(\frac{D\mathbf{z}}{Dt})^2 - \frac{D\mathbf{q}_J}{Dt} \qquad\qquad (4)$$

where $\mathbf{m}(x,z_2,z_3,z_4)$ is the added mass matrix of the ship section when the oscillating frequency tends to infinity; $D\mathbf{q}_J/Dt$ accounts for the hydrodynamic memory effect governed by the following set of differential equations

$$\frac{\partial \mathbf{q}_j}{\partial t} = \mathbf{q}_{j-1} - \mathbf{B}_{j-1}\mathbf{q}_J - (\mathbf{A}_{j-1} + \mathbf{B}_{j-1}\mathbf{m})\frac{D\mathbf{z}}{Dt} \qquad j = 1,2,...,J \tag{5}$$
$$\mathbf{q}_0 = 0$$

The third term of $\mathbf{F}(x,t)$ in Equation 4 provides the momentum slamming force. It vanishes in the linear problem. According to physical judgements, this term is usually only taken into account when the ship section enters into the water.

3. Current assumptions

There are some basic assumptions for the present problem as follows

(1) Neglect the effect of horizontal motions – surge, sway and yaw.

(2) Neglect hydroelastic effect on roll motion.

(3) Neglect the effect of the variation of wetted surface on rolling added mass and damping.

(4) Neglect the hydrodynamic coupling between roll and vertical motions. Coupling of roll motion with the vertical modes is introduced by hydrostatic restoring force and moments in heave, roll and pitch displacements.

Under the above assumptions, the hydrodynamics of the vertical and rolling motions can be treated separately. The motions will then be coupled through hydrostatic forces.

4. Non-linear time-domain hydroelastic vertical motions [2]

By incorporation of the hydrostatic action and rolling effect in Equation 4, the total vertical non-linear external fluid force acting on a ship section can be expressed as

$$Z(x,t) = -m\frac{D^2 z_3}{Dt^2} + U\frac{\partial m}{\partial x}\frac{Dz_3}{Dt} - \frac{\partial m}{\partial z}(\frac{Dz_3}{Dt})^2 - \frac{Dq_J}{Dt} + \rho g(S_0 + S_1) \tag{6}$$

where ρ is the density of the water and g is the gravitational acceleration. S_0 denotes the instantaneous immersed area of the ship section due to vertical motions. S_1 represents the increment of submerged area arising in rolling motions (Figure 2 and Appendix). For wall-sided hull forms this term will disappear, but for ships with flare, it may be significant

$$S_1(x) = \frac{1}{4}b_0^2(x)[\frac{dy}{dz} \times \tan^2(z_4)]/[1 - (\frac{dy}{dz})^2 \times \tan^2(z_4)] \tag{7}$$

where $b_0(x)$ is the breadth at the calm water line, dy/dz represents the section flare slope at the calm water line, and z_4 is the relative displacement between rolling motion and average wave slop across the section.

The hull is modelled as a linear elastic non-uniform Timoshenko beam. The assumption of small rigid-body motions and structural distortions allows model superposition of the displacement [2, 4]

$$w(x,t) = \sum_{r=0}^{n} w_r(x) p_r(t) \tag{8}$$

where w_r is the rth unit dry mode shape, and p_r the rth generalized principal coordinate of motion. In this analysis only the vertical response problem is consider. Therefore $r=0$ and 1 corresponds to heave and pitch motions, while $r=2,3,...,n$ represents elastic distortions of the hull girder.

The equation of motions for the ship hull can be written as

$$\sum_{r=0}^{n} [a_{sr}\ddot{p}_r(t) + b_{sr}\dot{p}_r(t) + c_{sr}p_r(t)] = \int_{L} (Z(x,t) - \mu g)w_s \, dx, \qquad s = 0,1,...,n. \tag{9}$$

Hereafter overdot denotes differentiation with respect to time. In this equation, $Z(x,t)$ is the total fluid action as represented by Equation 6, $\mu(x)$ the longitudinal distribution of mass of the ship structure, L the ship length, and a_{sr}, b_{sr}, c_{sr} are the components of the generalized structural mass, damping and stiffness matrices

$$a_{sr} = \delta_{sr} \int_{L} (\mu w_r w_s + I_y \theta_r \theta_s) \, dx$$
$$b_{sr} = \delta_{sr} a_{sr} \omega_r \alpha_r / \pi \tag{10}$$
$$c_{sr} = \delta_{sr} a_{sr} \omega_r^2$$

where δ_{sr} is the Kronecker delta function, I_y the longitudinal distribution of moment of inertia of the structure, θ_r the rth mode angular function of the ship hull girder beam in the x-z plane induced by vertical bending, α_r the rth mode logarithmic damping decrement of the structure in vacuum, and ω_r the rth mode eigenfrequency of the dry hull. In order to preserve the orthogonality between the rigid-body modes (heave and pitch), it is necessary that the mode shape $w_1(x)$ and x-axis intersect at the centre of mass of beam. It is assumed that the cross damping coefficients b_{sr} ($r{\neq}s$) can be neglected.

By substituting Equation 6 into Equation 9, the equations of the fluid structure interaction can be obtained as

$$(\mathbf{a} + \mathbf{A})\ddot{\mathbf{p}}(t) + (\mathbf{b} + \mathbf{B})\dot{\mathbf{p}}(t) + (\mathbf{c} + \mathbf{C})\mathbf{p}(t) = \mathbf{R} + \mathbf{W} + \mathbf{P} + \mathbf{Q}(\mathbf{q}) \tag{11}$$
$$\dot{\mathbf{q}}(x,t) = \mathbf{\Phi}\mathbf{q}(x,t) + \mathbf{\Psi}$$

with the initial conditions

$$\mathbf{p}(0) = \dot{\mathbf{p}}(0) = \mathbf{q}(x,0) = 0 \tag{12}$$

In the above equation, $\mathbf{p}$ is the generalized coordinate voter, $\mathbf{p}=\{p_0,p_1,...,p_n\}^T$, $\mathbf{q}$ is a voter used in the integration of the higher-order hydrodynamic equation, $\mathbf{q}=\{q_0,q_1,...,q_J\}^T$; $\mathbf{A,B,C}$ are the generalized fluid added mass, damping and restoring

force coefficients, which are functions of t and $\mathbf{p}$ in the non-linear problem, $\mathbf{R}(t;\mathbf{p})$ represents the generalized combined action of the instantaneous hydrostatic restoring force and the structural gravitational force, $\mathbf{W}(t;\mathbf{p})$ is the generalized non-linear wave diffraction force, $\mathbf{P}(t;\mathbf{p},\dot{\mathbf{p}})$ is the generalized 'momentum slamming' force; $\mathbf{Q}(\mathbf{q})$ is the generalize 'memorial' hydrodynamic force

$$A_{sr}(t;\mathbf{p}) = \int_L m w_r w_s \, dx$$

$$B_{sr}(t;\mathbf{p}) = -U \int_L m(w_r' w_s - w_s' w_r) \, dx - U m w_r w_s \big|_0^L$$

$$C_{sr}(t;\mathbf{p}) = -U^2 \int_L m w_r' w_s' \, dx + U^2 m w_r' w_s \big|_0^L$$

$$R_s(t;\mathbf{p}) = g \int_L [\rho(S_0 + S_1) - \mu] w_s \, dx$$

$$W_s(t;\mathbf{p}) = \int_L [m w_s (\ddot{\xi} - U \ddot{\xi}') + U m w_s' (\dot{\xi} - U \xi')] \, dx - U m w_s (\dot{\xi} - U \xi') \big|_0^L \tag{13}$$

$$P_s(t;\mathbf{p},\dot{\mathbf{p}}) = \int_L f_m w_s \, dx$$

$$f_m(x,t;\mathbf{p},\dot{\mathbf{p}}) = \begin{cases} \left| \dfrac{\partial m}{\partial z_3} \right| V^2 & V < 0 \\[2ex] 0 & V \geq 0 \end{cases}$$

$$Q_s(\mathbf{q}) = -\int_L (\dot{q}_J w_s + U q_J w_s') \, dx + U q_J w_s \big|_0^L$$

$$r, s = 0, 1, 2, \ldots, n.$$

In the above equations, prime indicates differentiation with respect to x. V is the relative vertical velocity between the section and the wave surface. The matrices $\mathbf{\Phi}$ and $\mathbf{\Psi}$ in Equation 11 are, respectively, expressed by

$$\mathbf{\Phi}(x,t;\mathbf{p}) = \begin{bmatrix} 0 & \cdots & 0 & 0 & -B_0 \\ 1 & \cdots & 0 & 0 & -B_1 \\ & & \vdots & & \\ 0 & \cdots & 1 & 0 & -B_{J-2} \\ 0 & \cdots & 0 & 1 & -B_{J-1} \end{bmatrix} \tag{14}$$

$$\mathbf{\Psi}(x,t;\mathbf{p},\dot{\mathbf{p}}) = \begin{Bmatrix} -(A_0 + m B_0)V \\ -(A_1 + m B_1)V \\ \vdots \\ -(A_{J-2} + m B_{J-2})V \\ 0 \end{Bmatrix} \tag{15}$$

5. Non-linear time-domain roll motion

The mathematical model employed in this study to describe the non-linear roll motion is of the form [5,6]

$$(I_x + A_{44})\ddot{\phi} + B(\dot{\phi}) + C(\phi, z_4) = W + Q(q) \tag{16}$$
$$\dot{q} = \Phi_r q - \Psi_r$$

with the initial conditions

$$\phi(0) = \dot{\phi}(0) = q(x,0) = 0 \tag{17}$$

where I_x is the mass moment of inertia with respect to x-axis, A_{44} is added inertia in roll. ϕ is the generalized coordinates corresponding to roll.

The damping moment is given as [6]

$$B(\dot{\phi}) = B_{44}\dot{\phi} + B_{444}|\dot{\phi}|\dot{\phi} \tag{18}$$

where B_{44} is the linear damping moment coefficient, and B_{444} is the quadratic damping moment coefficient.

The damping coefficients can be obtained from free decay experiments, in which the model is released from a given inclination angle to freely roll in calm water with no forward speed. It is assumed that the ship is under uncoupled roll motion during the free decay experiments. Then using appropriate curve parametric identification techniques, the coefficients B_{44} and B_{444} can be obtained by fitting equation to the recorded free decay experiment data [7]

$$(I_{xx} + A_{44})\ddot{\phi} + B_{44}\dot{\phi} + B_{444}\dot{\phi}|\dot{\phi}| + \Delta\overline{GM}\phi = 0 \tag{19}$$

where Δ is weight of water displaced by the ship. $\overline{GM}$ is metacentric height.

In present research, linear damping coefficient B_{44} was estimated by empirical formula [5]

$$B_{44} = 2d\sqrt{(I_x + A_{44})C_{44}} \qquad 0.08 \leq d(\beta) \leq 0.4 \tag{20}$$

$d(\beta) = 0.2$ was used in the calculations. The quadratic damping moment coefficient B_{444} was neglected.

The restoring moment is derived under the assumption that vertical motions due to amplitude waves are small, such that relative vertical displacement at a point of the length of the ship may be taken as the sum of two effects of heave and pitch motion. The roll restoring moment in waves is then given by [6]

$$C(\phi, z_4) = C_{44}\phi + C_{444}\phi^3 + C_{44z}\phi \tag{21}$$

where C_{44} and C_{444} represent linear and third order roll restoring coefficient [5]

$$C_{44} = g \int_L [\rho(\frac{b_0^2(x)}{12} + z_b S) - \mu z_g] dx \approx \Delta \overline{GM} \qquad (22)$$

where z_b is vertical position of buoyancy centre of the section.

C_{444} can be obtained from the hydrostatic curve of the ship [8]. It is neglected in present calculations.

C_{44z} represent time-dependent variation of hull restoring characteristic due to heave motion of a section (Figure 3), to second order [6],

$$C_{44z} = -\rho g \int_L [\frac{1}{2} b_0^2(x) \frac{dy}{dz} - z_g b_0(x)] z_3 dx \qquad (23)$$

where the definition of $b_0(x)$ and dy/dz are the same as in Equation 7. z_g is vertical coordinate of ship centre of gravity, z_3 is the relative vertical displacement between a ship section and the wave surface.

In equation 17, $q(x,t)$ is a variation used in the integration of the higher-order hydrodynamic equation; $W(t)$ is the generalized wave force and $Q(q)$ is the generalized hydrodynamic 'memory' force.

6. Numerical methods [2, 3]

The second-order central difference scheme is used to determine the eigenvalues and principal modes of the free-free non-uniform Timoshenko beam. The modes of displacement w_r, bending slope, shearing angle, bending moment M_r, shearing force V_r and the natural frequencies ω can be simultaneously obtained through an iterative procedure with very small computational effort.

A multi-parameter conformal transformation technique is used to solve the vertical two-dimensional frequency-domain hydrodynamic coefficients (added mass and added damping) of the sections at several draughts. The singularity distribution method is used to determine the two-dimensional frequency-domain hydrodynamic coefficients for roll motion.

Equation 3 is exactly satisfied at *2J-1* frequencies. In order to achieve the best approximation within a given frequency range, the frequency-independent hydrodynamic coefficients A_j and B_j are obtained by minimizing

$$\sum_{r=1}^{K} \{\text{Re}(\varepsilon_r)^2 + \text{Im}(\varepsilon_r)^2\} \qquad (24)$$

with

$$\varepsilon_r = \sum_{j=0}^{J} (i\omega_r)^j [A_{j,k} + (m_k - \frac{iN_k}{\omega_r}) B_{j,k}] \qquad k = 3,4 \qquad (25)$$

where ω_r are discrete circular frequencies within the given ship-dependent frequency range. From numerical tests it is found that, in order to reach good agreement between the original and the approximated frequency-domain hydrodynamic coefficients, a third-order differential approach ($J=3$) is necessary and sufficient for most sectional shapes except for roll of the extreme U-shaped sections (Figure 4). In this case, the twin peak appears in the frequency response of damping (Figure 5). It is difficult to approximate correctly for the whole frequency range by third-order (or even higher-order) differential approach. In order to get a more reasonable approximation, added damping was only approximated in higher frequency range because the damping in low frequency is much smaller than that in high frequency (Figure 6).

The non-linear differential equations for the coupled fluid-structure system are integrated in the time domain by using the Adams predictor-corrector scheme. The fourth-order Runge-Kutta method is used to predict the function values at the previous four time steps.

7. Calculations for a Panamax Container Ship

Time-domain simulations are performed for a Panamax Container Ship. A detailed description of the experiments including the body plan and the main particulars of the ship can be found in Tan [9].

The uncoupled results have been compared with model tests. The agreement is acceptable for the linear roll motion and non-linear vertical modes [3,5].

Considering the harmonic character of time varying terms, the equations 11 and 17 are recognized as forming a set of coupled Mathieu equations. This type of system of ordinary differential equations with periodic coefficients may be, in general, subjected to parametric resonance for encounter frequencies close to [10]

$$\mathrm{m}\omega_e = \omega_i \pm \omega_j, or, 2\omega_i, \qquad m = 1,2,..., \qquad i,j = 3,4,5 \qquad (26)$$

For the Panamax Container Ship, the nature frequencies of heave, roll and pitch are $\omega_3=0.73\ rad/s$, $\omega_4=0.25\ rad/s$, and $\omega_5=0.73rad/s$, respectively.

Following the above analyses, the simulations are conducted for three wave headings: $\beta=15,\ 90,\ 165$ degrees (180 degrees denote head waves). For each wave heading, two encounter frequencies, which probably lead to parametric resonance, are considered. The range of wavelength to ship length ratio is: $\lambda/L=0.5\sim2.5$. The wave amplitude was kept constant at 5 m. Ship speed is 24.5 knot.

The computational results are showed in Figure 7 to 12. For each time series, uncoupled results are also given.

Figure 7 and 8 give the results for wave heading $\beta=15°$ and encounter frequencies $\omega_e=0.12\ rad/s$ ($4\omega_e=\omega_3-\omega_4$) and $\omega_e=0.16\ rad/s$ ($3\omega_e=\omega_3-\omega_4$). In Figure 7, amplitudes of uncoupled roll responses are of the order of 4 degrees; the roll response from the coupled set of equations is of the order of 13 degrees. Much large coupled roll motions are found in this condition. Coupled heave and pitch are also very different

from the uncoupled solution, but these motions are small in amplitudes. In Figure 8, coupled roll motion is not very different from uncoupled motions. Coupled heave and pitch motions are nearly the same as uncoupled motions.

Figure 9 and 10 present the results from the beam waves. The encounter frequencies are $\omega_e=0.49$ *rad/s* $(2\omega_e=\omega_3+\omega_4)$ and $\omega_e=0.3266$ *rad/s* $(3\omega_e=\omega_3+\omega_4)$. In this case, coupled pitch motions change a lot. The effects of coupled motions are bigger in lower frequency than that in higher frequency. Both coupled and uncoupled pitch motions are small in amplitude. Coupled heave and roll motions are not very different form uncoupled motions.

Figure 11 and 12 show the results for the bow waves (wave heading $\beta=165°$). The encounter frequencies are $\omega_e=0.98$ *rad/s* $(\omega_e=\omega_3+\omega_4)$ and $\omega_e=0.48$ *rad/s* $(\omega_e=\omega_3-\omega_4)$. The coupled heave and pitch motions are nearly the same as uncoupled motions. The mean values of coupled roll motions are biased. It may be due to the bias of pitch motions. Both coupled and uncoupled roll motions are small.

It is seen from these comparisons that parametric instability occurs when the ship sails in quartering waves and very low encounter frequency. In other computational wave conditions, the effects of coupling of heave, pitch and roll are small.

8. Concluding remarks

The time-domain strip theory for vertical and rolling motions has been extended to predict the coupling of heave, pitch and roll motions by combining hydrostatic restoring force and moments in heave, pitch and roll displacements. Corresponding computer program has been developed.

Time-domain simulations were performed for a Panamax Container ship at different headings and encounter frequencies. The coupling effect and parametric resonance were investigated.

Acknowledgements

References

[1] Neves, M.A.S., Valerio, L., 2000. Parametric resonance in waves of arbitrary heading. 7th International Conference on Stability of Ships and Ocean Vehicles, Tasmania, Australia, 680-687.

[2] Xia, J., Wang, Z, Jensen, J., 1998. Non-linear wave loads and ship responses by a time-domain strip theory. Marine Structures 11(3), 101-123.

[3] Wang, Z., 2000. Hydroelastic analysis of high speed ships. Ph.D. Thesis, Department of Naval Architecture and Offshore Engineering, Technical University of Denmark.

[4] Bishop, R.E.D., Price, W.G., 1979. Hydroelastict of ships, Cambridge University Press.

[5] Wang, Z, Jensen, J., Xia, J., 2001. Prediction of wave-induced rolling responses by a time-domain strip theory. PRADS, Shanghai.

[6] Neves, M.A.S., Perez, N.A., Valerio, L., 1999. Stability of small fishing vessels in longitudinal waves. Ocean Engineering 26, 1389-1419.

[7] Silva, S.R., Soares, C.G., 2000. Time domain simulation of parametrically excited roll in head seas. 7th International Conference on Stability of Ships and Ocean Vehicles, Tasmania, Australia, 652-664.

[8] Ouyang, R, 1999. Application of bifurcation theory and numerical method in stability of marine vehicle. Ph.D. These, Shanghai Jiao Tong University, (in Chinese).

[9] Tan, S.G., 1972. Wave load measurements on a model of a large container ship, Netherlands Ship Research Center, Report 173S.

[10] Cesari, L., 1971. Asymptotic behavior and stability problems in ordinary differential equations, Third Edition, Springer-Verlag, 65-80.
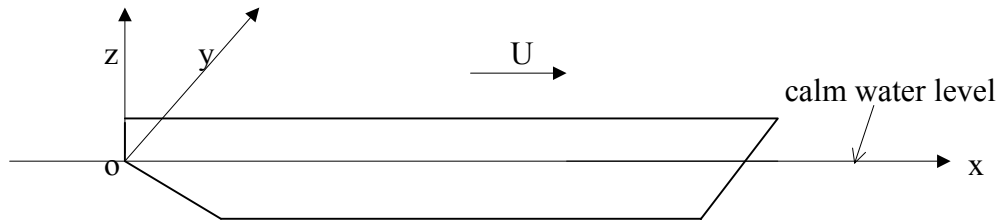
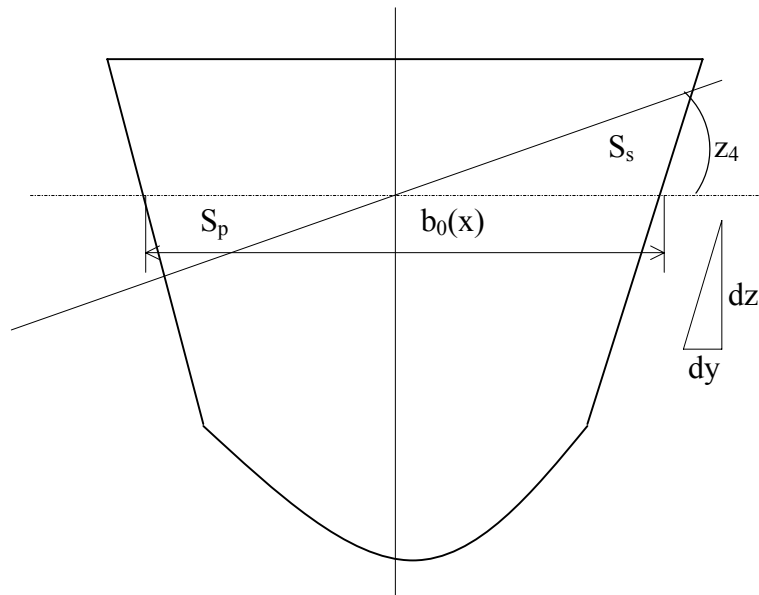Figure 1 Equilibrium coordinate system

Figure 2 Effect of roll on heave for a unit section
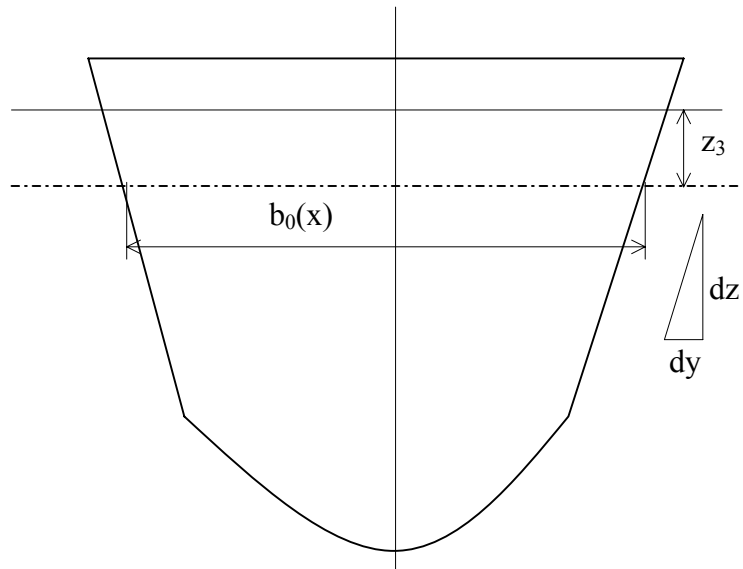Increment of vertical restoring force $\Delta Z = \rho g(S_s - S_p)$

Figure 3 Variation of sectional beam with relative vertical displacement
Roll hydrostatic moment coefficient changes with
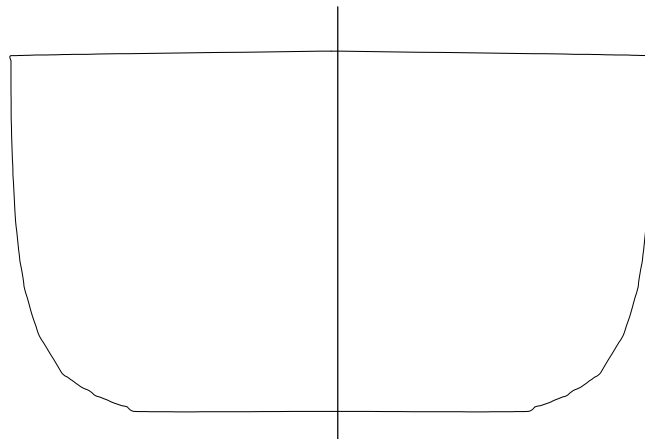the change of inertia, area centre and submerged volume
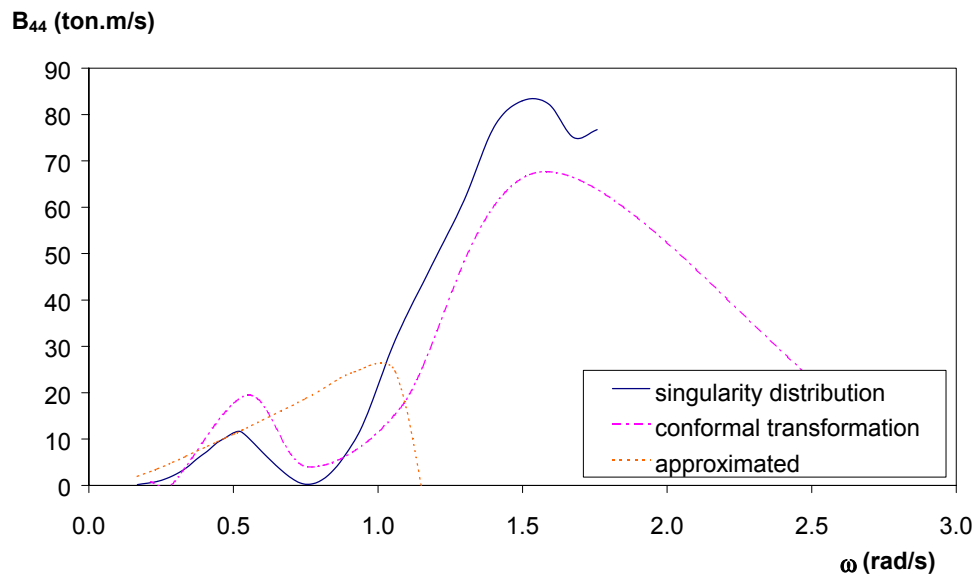

Figure 4 Section plan of #10 station

B$_{44}$ (ton.m/s)

Figure 5 Comparison of the damping calculated by different methods

B$_{44}$ (ton.m/s)
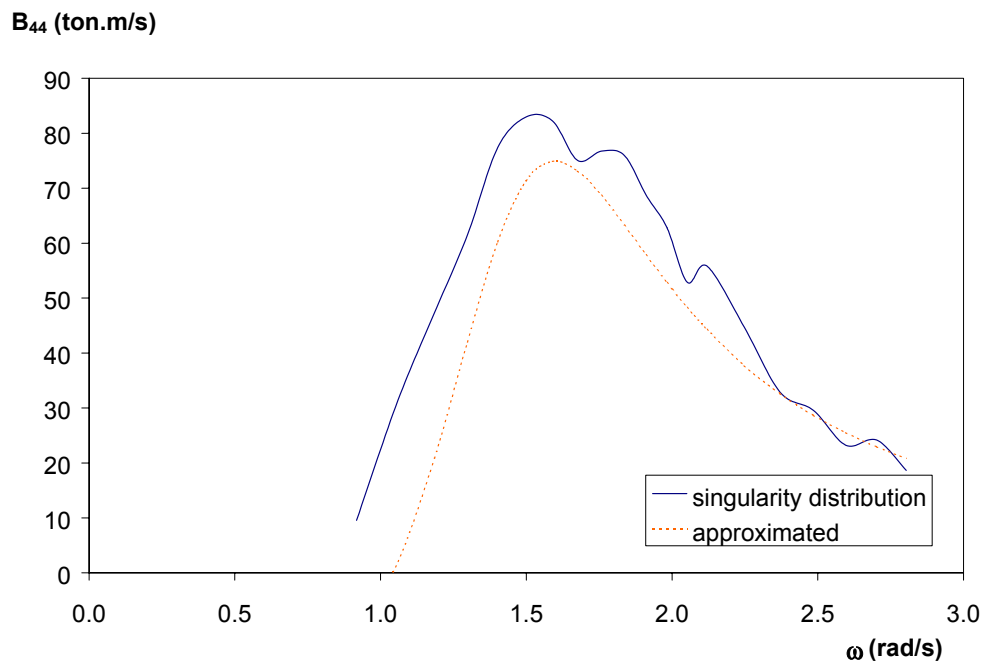
Figure 6 Damping approximated by changing the range of frequency
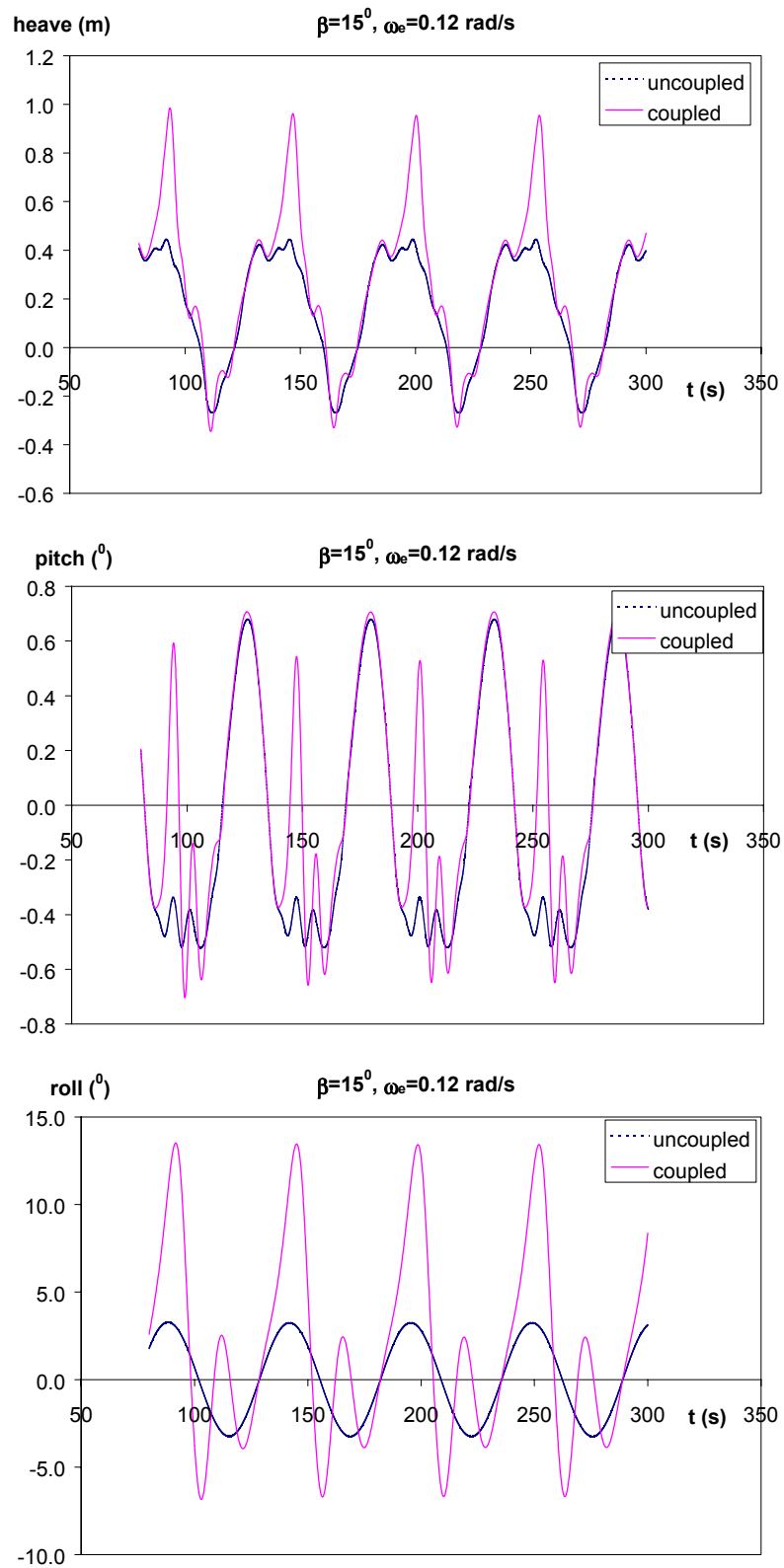
Figure 7 Simulated motions
(wave heading $\beta=15°$, encounter frequency $\omega_e=(\omega_3-\omega_4)/4$)
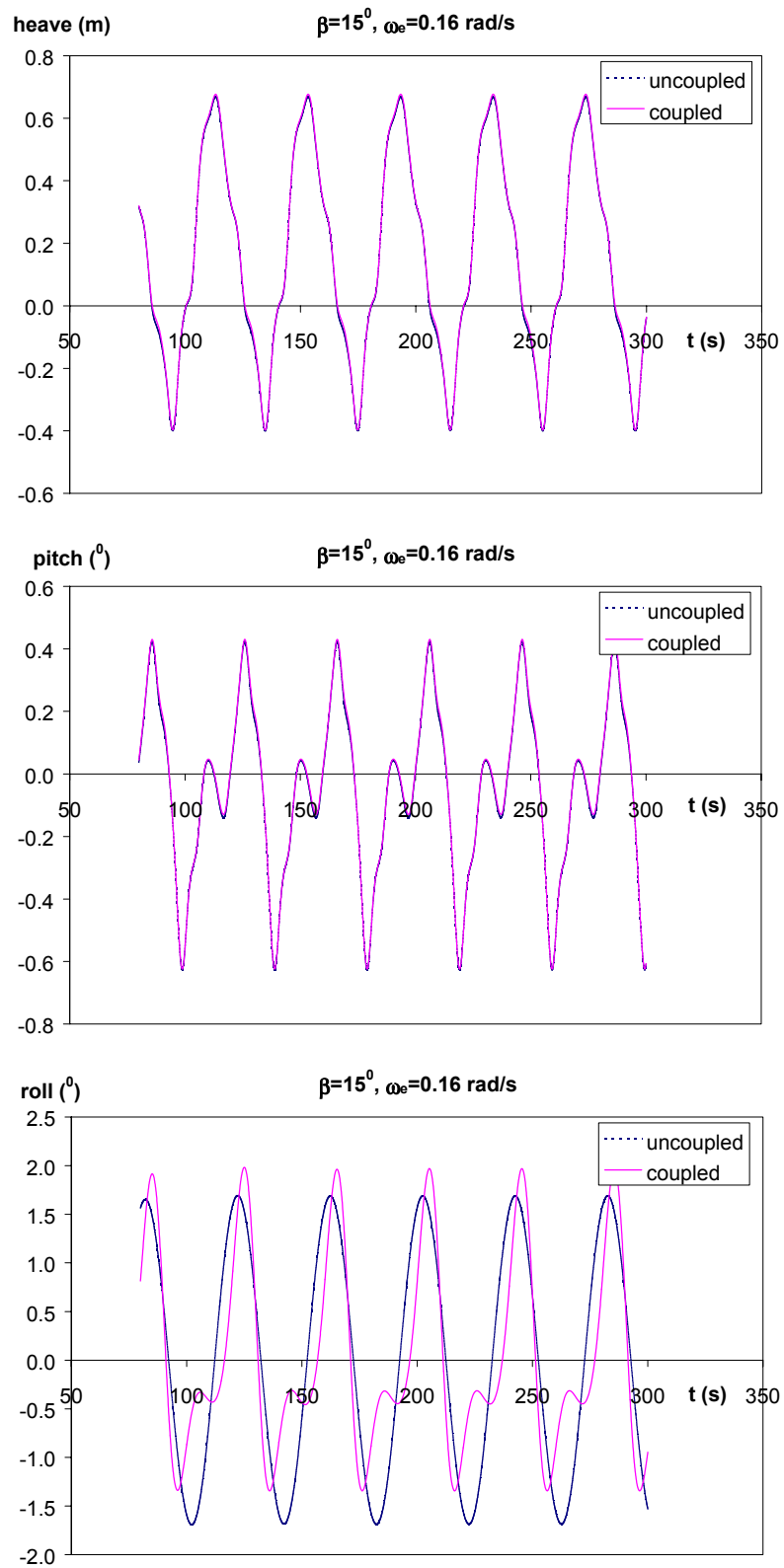
Figure 8 Simulated motions
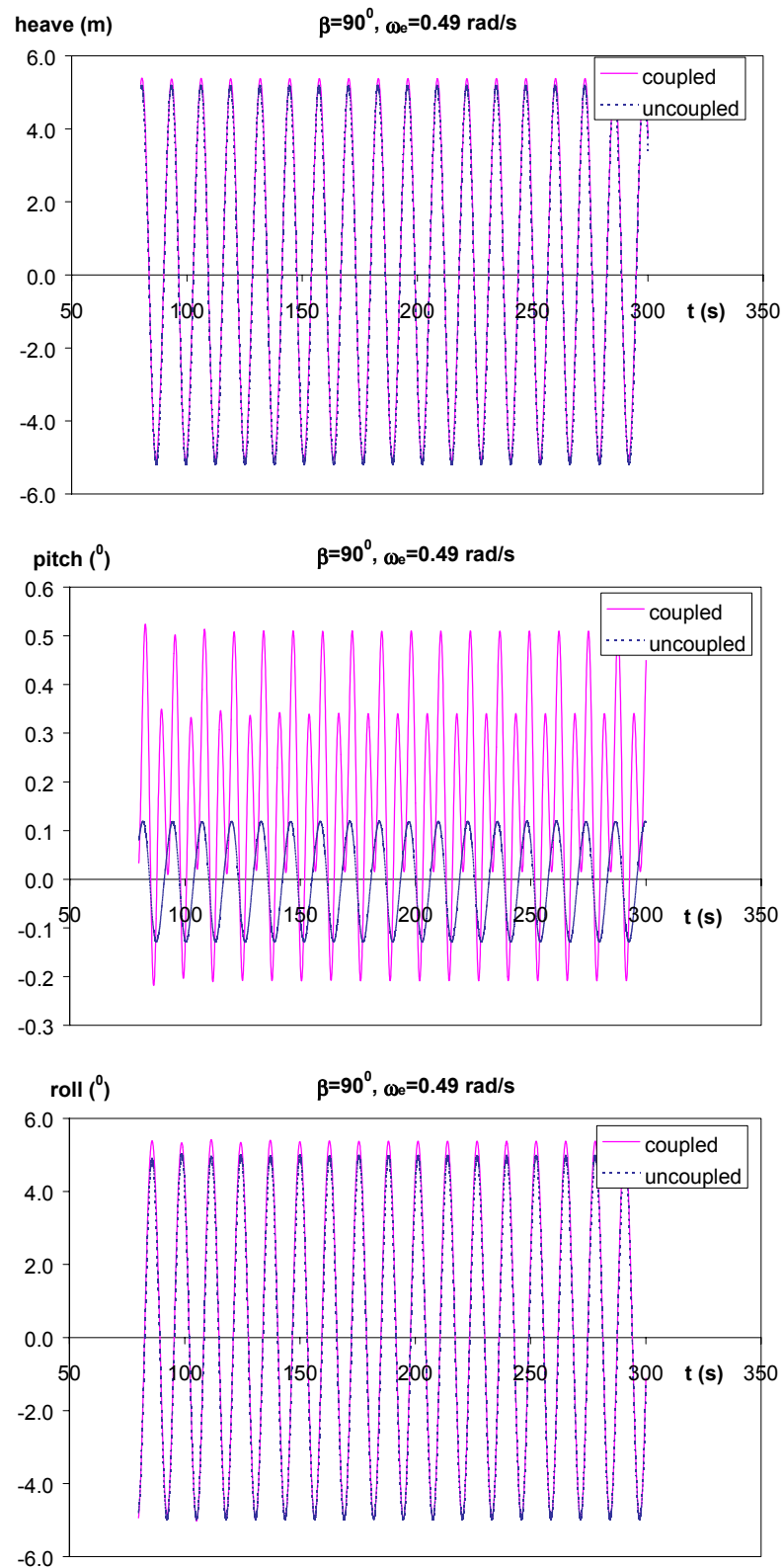(wave heading $\beta=15°$, encounter frequency $\omega_e=(\omega_3-\omega_4)/3$)

Figure 9 Simulated motions
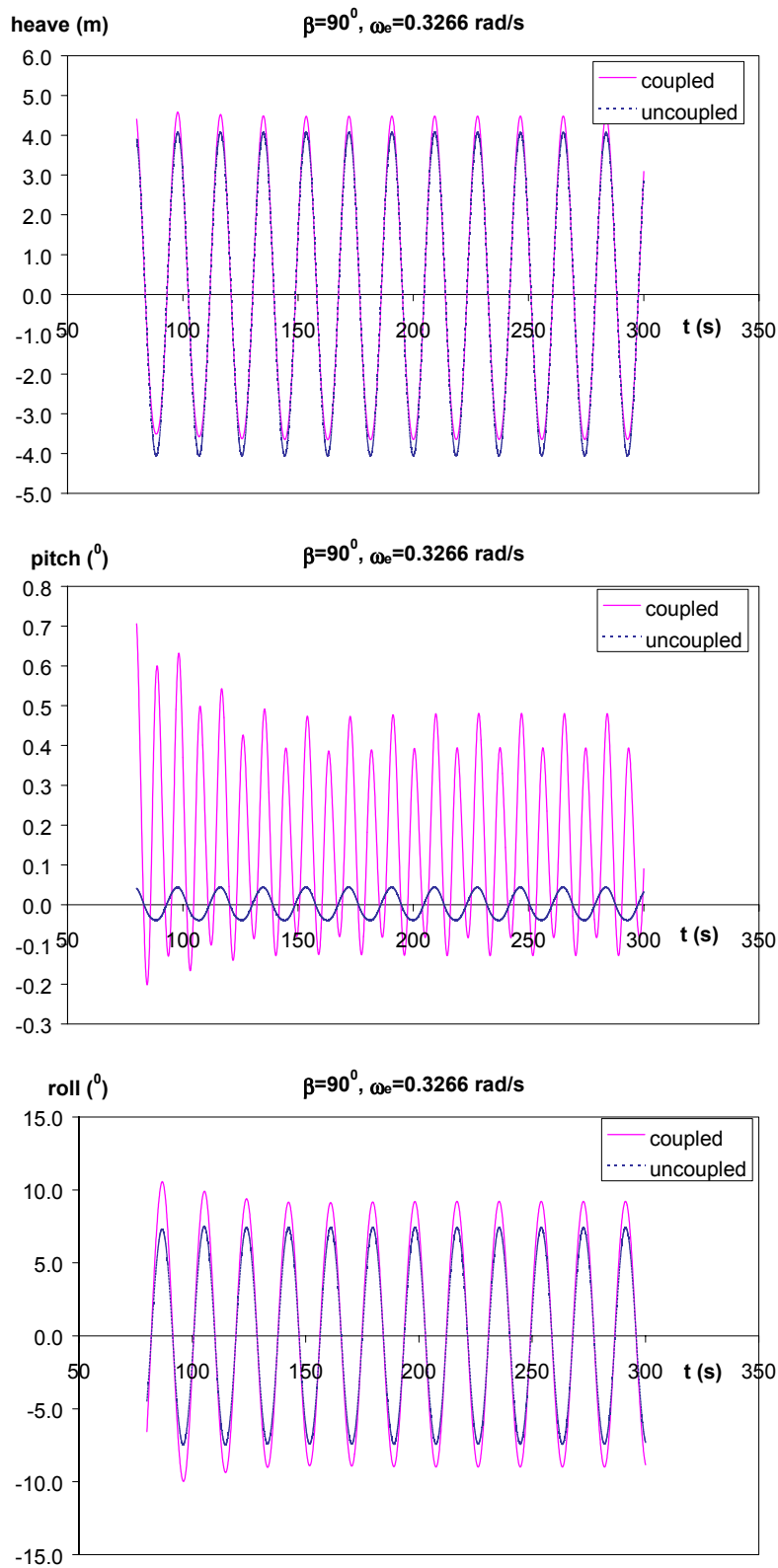(wave heading $\beta=90°$, encounter frequency $\omega_e=(\omega_3+\omega_4)/2$)

Figure 10 Simulated motions
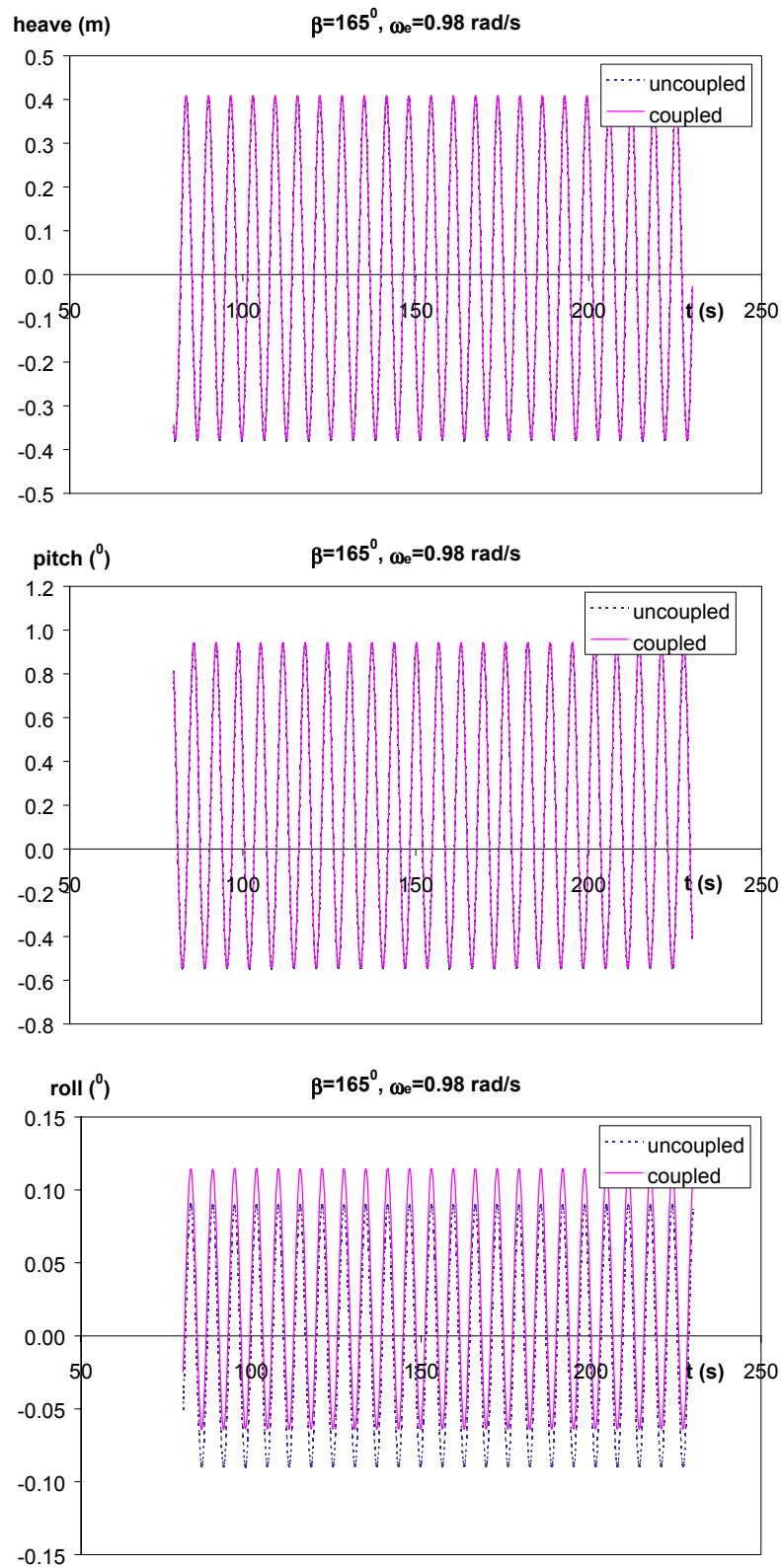(wave heading $\beta=90°$, encounter frequency $\omega_e=(\omega_3+\omega_4)/3$)

Figure 11 Simulated motions
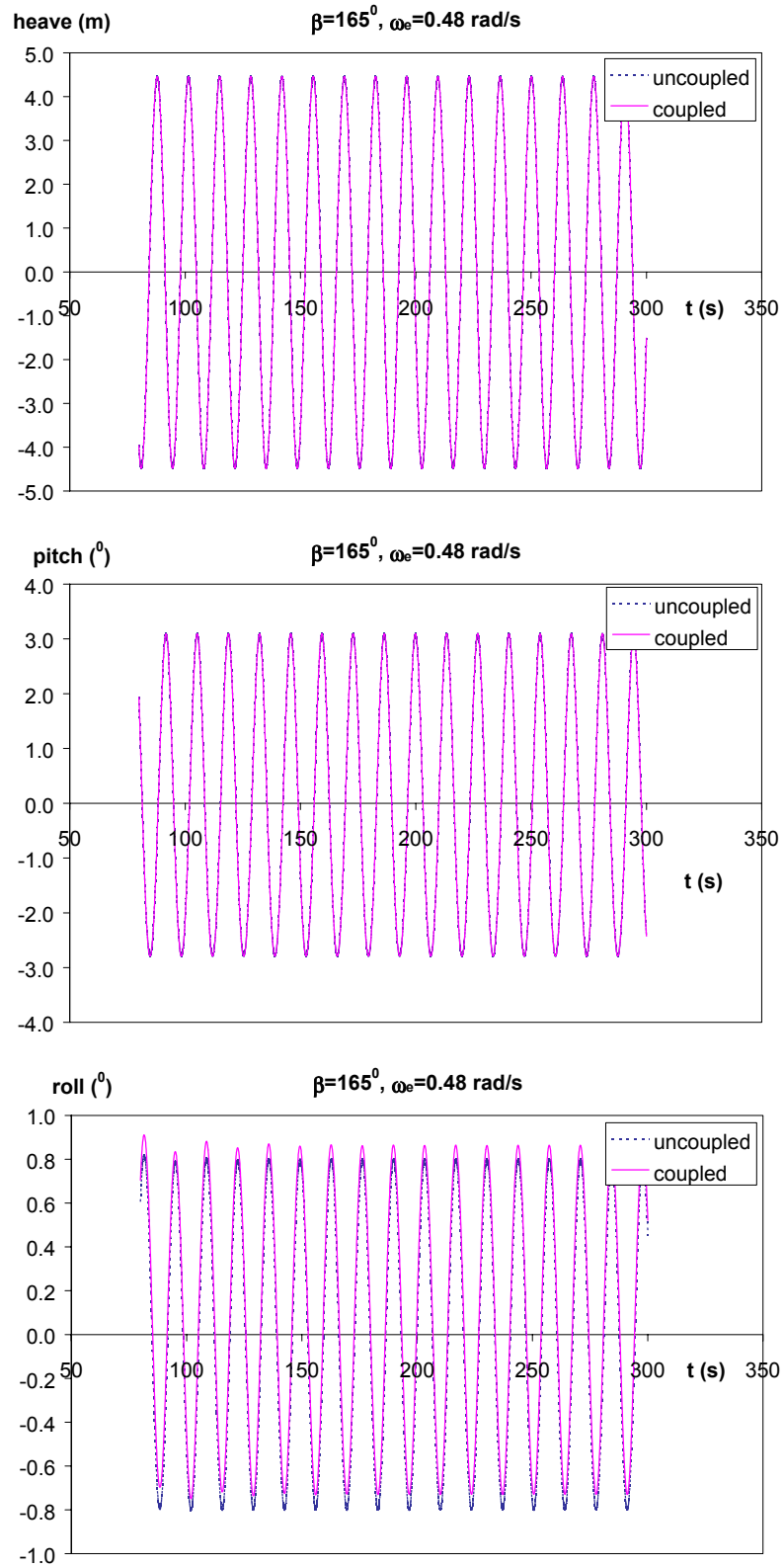(wave heading β=165°, encounter frequency $\omega_e=(\omega_3+\omega_4)$)

Figure 12 Simulated motions
(wave heading $\beta=165°$, encounter frequency $\omega_e=(\omega_3-\omega_4)$)

Appendix The derivation of Equation 7

In Figure 2, the areas of S_S and S_P can be express as

$$S_S = \frac{1}{8} b_0^2(x) \frac{\tan(z_4)}{1 - \frac{dy}{dz}\tan(z_4)}$$

$$S_P = \frac{1}{8} b_0^2(x) \frac{\tan(z_4)}{1 + \frac{dy}{dz}\tan(z_4)}$$

The increment of immerged area of the section is

$$S_1 = S_S - S_P = \frac{1}{4} b_0^2(x)[\frac{dy}{dz} \times \tan^2(z_4)]/[1 - (\frac{dy}{dz})^2 \times \tan^2(z_4)]$$